Fabrication of 3D hepatic tissues by additive photopatterning of cellular hydrogels

Valerie Liu Tsang,* Alice A. Chen,† Lisa M. Cho,* Kyle D. Jadin,* Robert L. Sah,* Solitaire DeLong,‖ Jennifer L. West,‖ and Sangeeta N. Bhatia*,†,‡,§,1

*Department of Bioengineering, University of California, San Diego, La Jolla, California, USA; †Harvard-Massachusetts Institute of Technology Division of Health Sciences and Technology, and ‡Department of Electrical Engineering and Computer Science, §Division of Medicine, Brigham and Women's Hospital, Boston, Massachusetts, USA; Massachusetts Institute of Technology, Cambridge, Massachusetts, USA; and ‖Department of Bioengineering, Rice University, Houston, Texas, USA

ABSTRACT **We have fabricated a hepatic tissue construct using a multilayer photopatterning platform for embedding cells in hydrogels of complex architecture. We first explored the potential of established hepatocyte culture models to stabilize isolated hepatocytes for photoencapsulation (*e.g.*, double gel, Matrigel, cocultivation with nonparenchymal cells). Using photopolymerizable PEG hydrogels, we then tailored both the chemistry and architecture of the hydrogels to further support hepatocyte survival and liver-specific function. Specifically, we incorporated adhesive peptides to ligate key integrins on these adhesion-dependent cells. To identify the appropriate peptides for incorporation, the integrin expression of cultured hepatocytes was monitored by flow cytometry and their functional role in cell adhesion was assessed on full-length extracellular matrix (ECM) molecules and their adhesive peptide domains. In addition, we modified the hydrogel architecture to minimize barriers to nutrient transport for these highly metabolic cells. Viability of encapsulated cells was improved in photopatterned hydrogels with structural features of 500 μm in width over unpatterned, bulk hydrogels. Based on these findings, we fabricated a multilayer photopatterned PEG hydrogel structure containing the adhesive RGD peptide sequence to ligate the $\alpha_5\beta_1$ integrin of cocultured hepatocytes. Three-dimensional photopatterned constructs were visualized by digital volumetric imaging and cultured in a continuous flow bioreactor for 12 d where they performed favorably in comparison to unpatterned, unperfused constructs. These studies will have impact in the field of liver biology as well as provide enabling tools for tissue engineering of other organs.—Liu Tsang, V., Chen, A. A., Cho, L. M., Jadin, K. D., Sah, R. L., DeLong, S., West, J. L., Bhatia, S. N. Fabrication of 3D hepatic tissues by additive photopatterning of cellular hydrogels. *FASEB J.* 21, 790–801 (2007)**

Key Words: tissue engineering · liver · hepatic · PEG · microscale

Tissue engineering of an implantable liver construct faces many obstacles due to the highly metabolic nature and diverse set of functions of the liver. Previous studies in this field have explored options such as hepatocyte attachment to microcarriers (1), encapsulation of hepatocyte aggregates (2, 3), and biodegradable polymer scaffolds (4–6). Transplantation of hepatocytes (preaggregated or attached to protein-coated microcarriers) has been shown to provide initial function, but their potential for prolonged efficacy has not been demonstrated (7). The high metabolic rate of hepatocytes presents transport limitations as diffusive nutrient transport is only sufficient over short length scales. As a result, methods have been developed to generate scaffolds with architectural features that allow convective perfusion; however, acellular scaffolds can be difficult to populate with cells that are really nonproliferative and nonmotile *in vitro*, like hepatocytes (8). Proposed solutions to this challenge include dynamic seeding of constructs by perfusion with cell suspensions or fabrication of channels in vascular-mimetic patterns (9–11). Others have incorporated growth factors into scaffolds seeded with hepatocytes to promote engraftment and angiogenesis, resulting in improvements in microvascular density and hepatocyte engraftment over controls (12, 13). Despite these innovations, to date hepatocytes transplanted into rats on biodegradable polymer matrices are still found to be inferior to liver grafts of equivalent liver mass in compensating for metabolic deficiencies (14). Thus, methods of building tissue engineered liver constructs with intricate architectures that provide adequate transport of oxygen and nutrients as well as an environment that promotes hepatocyte viability and liver-specific function are still lacking.

In recent years, rapid prototyping manufacturing technologies have been applied toward the fabrication of three-dimensional scaffolds with tunable micro- and macroscale features (15–26). Synthetic hydrogels as a class of biomaterials have also been of increasing interest in tissue engineering because they can be tailored

[1] Correspondence: Massachusetts Institute of Technology, 77 Massachusetts Ave., E19–502D, Cambridge, MA 02139, USA. E-mail: sbhatia@mit.edu

doi: 10.1096/fj.06-7117com

0892-6638/07/0021-0790 © FASEB

for specific applications (adhesive regions, biodegradable linkages, *etc.*) and can be used to entrap cells at tissue-like densities. The transport properties of hydrogels can also be customized by adjusting polymer chain lengths and density. In particular, poly(ethylene glycol) (PEG)-based hydrogels have been widely utilized because of their biocompatibility, hydrophilicity, and ability to be chemically tailored (27). They have been explored to immobilize various cell types, including chondrocytes (28–30), vascular smooth muscle cells (31), osteoblasts (32), neural cells (33), and fibroblasts (34–36), which can attach, grow, and produce matrix, as well as progenitor cells, which can differentiate into adipose tissue (37) or cartilage tissue (38). PEG-based hydrogels have also been customized by incorporation of adhesion domains of ECM proteins to promote cell adhesion, growth factors to modulate cell function, and both hydrolytic and protease-sensitive linkages (31, 35, 39–45).

Photoencapsulation in PEG hydrogels combined with multilayer fabrication methods, therefore, represents a potential opportunity for hepatic tissue engineering (46). In this study, we combine the use of PEG hydrogels with photolithographic methods to fabricate hepatic tissues that enable high-density encapsulation while specifying scaffold architecture that enables nutrient delivery by convective flow. We first optimize conditions to incorporate hepatocytes in PEG hydrogels by stabilizing primary hepatocytes in culture and incorporating adhesive peptides to ligate hepatocyte integrins. Next, we photopattern single-layer hydrogel structures that incorporate hepatocytes at high density to reduce diffusive nutrient transport limitations. We subsequently fabricate and image multilayer 3D tissue structures with defined scaffold architecture. Finally, we perfuse these 3D tissue structures in a continuous-flow bioreactor and demonstrate improved viability and liver-specific function of the encapsulated hepatocytes over unpatterned controls.

MATERIALS AND METHODS

Cell culture

Cell sources and maintenance

Hepatocytes were isolated from 1- to 2-month-old adult female Lewis rats (Charles River Laboratories, Wilmington, MA, USA) weighing 50–150 g, by a modified procedure of Seglen (47). Detailed procedures for isolation and purification of hepatocytes were previously described by Dunn *et al.* (48). Routinely, 150–250 million cells were isolated with viability between 85% and 95%, as judged by trypan blue exclusion. Nonparenchymal cells, as judged by their size (<10 μm in diameter) and morphology (nonpolygonal or stellate), were less than 1%. Culture medium was Dulbecco's modified Eagle medium (DMEM; Life Technologies, Inc., Grand Island, NY, USA) supplemented with 10% FBS (Sigma, St. Louis, MO, USA), 0.5 U/mL insulin, 1.5 μg/mL glucagon, 7.5 μg/mL hydrocortisone, 100 U/mL penicillin, and 100 μg/mL streptomycin.

NIH 3T3-J2 cells were the gift of Howard Green, Harvard Medical School. Cells grown to preconfluence were passaged by trypsinization in 0.01% trypsin (ICN Biomedicals, Costa Mesa, CA, USA)/0.01% EDTA (Boehringer Mannheim, Indianapolis, IN, USA) solution in PBS for 5 min, diluted, and then inoculated into a fresh tissue culture flask. Cells were passaged at preconfluency no more than 16 times. Cells were cultured in 175 cm^2 flasks (Fisher Scientific, Springfield, NJ, USA) at 5% CO_2, balance moist air. Culture medium consisted of DMEM (Life Technologies, Inc.) with high glucose (Glc), supplemented with 5% bovine calf serum (BCS, JRH Biosciences, Lenexa, KS, USA) and 100 U/mL penicillin and 100 μg/mL streptomycin. Prior to use, the cells were growth-arrested by incubating in medium with 2 mg/mL Mitomycin C for 2 h so that they would not overgrow the coculture dishes.

Hepatocyte preconditioning and retrieval for flow cytometry and adhesion experiments

For integrin characterization and adhesion experiments, hepatocytes were cultured in one of three conditions: double gel, Matrigel, and coculture with fibroblasts. In addition, Day 0 hepatocytes were obtained from the pool of freshly isolated hepatocytes. Hepatocytes cultured in the double gel, or "sandwich configuration", were cultured between two 0.5 mm layers of collagen gel (49). Matrigel gel layers of 0.5 mm thickness consisted of Matrigel Basement Membrane Matrix (BD Discovery Labs, Bedford, MA, USA). Hepatocytes in the coculture condition were seeded on adsorbed collagen and allowed to adhere and spread, and an equal ratio of growth-arrested NIH 3T3-J2 fibroblasts were added on day 1. All cultures were maintained in the hepatocyte growth medium, which was replaced daily.

Cells were removed from culture after 1, 4, and 7 d of culture. Hepatocytes seeded in the double gel configuration were released by incubating the dishes with 5 ml of collagenase (Sigma, 2.68 mg/mL in 5mM $CaCl_2$ in KRB buffer) for 30–40 min at 37°C. BD Cell Recovery solution (BD Discovery Labs) was used to dissolve the Matrigel substrate by incubation for 1 h on ice. Cells in the coculture condition were released by washing with serum-free medium, treating with 0.05% trypsin/EDTA for 2 min to separate cells from each other and release fibroblasts, washing with medium containing serum to inactivate the trypsin, and finally incubating with 5 ml collagenase solution to release the cells from the dish (50). Large clumps of cells were removed by passing the cell suspensions through 70 μm mesh cell strainers (BD Biosciences) and washed with culture medium by centrifugation (50 *g* for 5 min at 4°C).

Cell preparation for hydrogel photopatterning

For 3D tissue fabrication, hepatocytes were maintained in coculture with fibroblasts. P-150 culture dishes were each plated with 7.5 million hepatocytes. Coculture dishes were cultured with an equal number of fibroblasts at the time of seeding. Removal of cells from culture was accomplished by 0.25% trypsin/EDTA with shaking. Some cells were fluorescently labeled with chloromethylfluorescein diacetate (CMFDA; C-2925, Molecular Probes, Eugene, OR, USA), chloromethylbenzoylaminotetramethyl rhodamine (CMTMR; C-2927, Molecular Probes), or 7-amino-4-chloromethylcoumarin (CMAC, C-2110, Molecular Probes) for identification at (ex/em) 492/517, 514/565, or 353/466 nm wavelengths, respectively.

Cell number within the patterned hydrogel construct was determined by calculating the vol of each layer based on the

geometry of the masks and by specifying the concentration of hepatocytes in the prepolymer solution. The vol of the hydrogel construct was determined to be ~50 μl. Therefore, the unpatterned gel (same overall thickness and diameter, but no photopatterning) was fabricated by tuning the hepatocyte concentration in the prepolymer solution to achieve the same number of hepatocytes (4×10^5 cells).

Flow cytometry for integrin characterization

Cells (0.25×10^6) were added to each FACS tube and washed with 1 ml FACS buffer (1% FBS, 0.1% sodium azide in PBS) by centrifugation. Primary antibodies used for flow cytometry were as follows: Armenian hamster IgG α_1, α_2, α_5, hamster IgG isotype control (BD Pharmingen, San Diego, CA, USA), Armenian hamster IgM $\beta_1$and hamster IgM istoype control (Pharmingen), mouse IgG α_4 and mouse IgG isotype control (Pharmingen), mouse α_3 (Ralph 3.1 developed by Louis Reichardt, obtained from the Developmental Studies Hybridoma Bank, developed under the auspices of the NICHD and maintained by the University of Iowa, Department of Biological Sciences), mouse $\alpha_6\beta_1$ (Biosource, Caramillo, CA, USA), rabbit α_9 (clone 1057, kindly provided by Dean Sheppard, Department of Medicine, UCSF), α_V (Chemicon, Temecula, CA, USA) and rabbit IgG isotype control (Southern Biotech, Birmingham, AL, USA). Diluted primary antibody (Ab; 100 μl; 1:100 in FACS buffer) was added to each tube of cells and allowed to incubate on ice for 15 min. Because the α_9 and α_V antibodies ligate the cytoplasmic domain of the integrin subunit, the cells were first permeabilized in a 50% ethanol solution (1 ml cell culture medium, 1 ml FBS, 6 ml 70% ethanol) by incubating on ice for 30 min and washed with FACS buffer before incubation with primary Ab, according to a protocol previously reported (51). All cells were washed by adding 1 ml FACS buffer and centrifuging at 500 rpm for 5 min at 4°C.

Secondary antibodies used were mouse antihamster IgG FITC (Pharmingen), mouse antihamster IgM FITC (Pharmingen), goat anti-mouse IgG FITC (Jackson Labs), and goat anti-rabbit IgG FITC (Sigma). The appropriate secondary antibodies (100 μl, diluted in FACS buffer, 1:100 for hIgG, mIgG, and rIgG, and 1:200 for hIgM) were added to cells and allowed to incubate on ice for 15 min. The cells were washed in 1 ml FACS buffer and then resuspended in 300 μl of FACS buffer. The analysis was performed using a FACScan flow cytometer (Becton Dickinson, Fullerton, CA, USA). Cells (5000 or 10,000) were analyzed for each sample.

Integrin expression was analyzed using FACS for hepatocytes from two rats. In the first experiment, all integrin antibodies were analyzed for all culture conditions. Integrin subunits α_2 and α_4 were not expressed in any conditions at any time points, and therefore were not used in the second experiment. Expression of α_1, α_3, α_5, α_6, α_9, and α_V were studied in both experimental runs.

Matrix adhesion studies

Cells were cultured in and released from common culture conditions (double gel, coculture with fibroblasts, Matrigel) and then added to matrix-coated culture plates to determine whether preculturing of cells affects adhesion and spreading onto certain surfaces. Human laminin, fibronectin, vitronectin, and collagen I coated plates were obtained from BD Discovery Labs. BSA-coated wells were used as a negative control. The cells were shaken gently every 15 min for 1 h and were allowed to adhere for 4 h. The wells were then washed three times with PBS to remove nonadherent cells. Tris-EDTA buffer (Sigma) was added to all wells, which were stored at –20°C until the time of assay. The PicoGreen DNA assay (Molecular Probes, Eugene, OR, USA) was used to quantify the number of cells attached in each well. Cells were subjected to three freeze/thaw cycles followed by ultrasonication, prepared in multiwell format with calf thymus DNA, and interrogated on a SpectraMAX GeminiXS spectrofluorometer (Molecular Devices, Sunnyvale, CA, USA) with ex/em of 485/530 nm. An average amount of 10 pg DNA per hepatocyte was used to estimate cell number.

Peptide film adhesion studies

The peptides RGDS, RGES, and YIGSR were obtained from Sigma. KQAGDV, GF[Hyp]GER, and cyclic (-RGD[D-Phe]K-) were synthesized by Global Peptide Corp. Conjugation of peptides to acryloyl-PEG-NHS and subsequent reaction characterization were performed using a protocol previously described (31, 35). The resulting monomers consisted of PEG chains flanked on one side by the desired peptide and on the other by an active acrylate group.

Peptide hydrogel solutions were created by combining desired concentrations of the PEG monoacrylate-Peptide with poly(ethylene glycol) diacrylate (PEGDA) (MW 3400, Nektar Transforming Therapeutics, Huntsville, AL, USA) and dissolving in PBS to form a 20% w/v solution. The photoinitiator 2,2-dimethoxy-2-phenyl-acetophenone (Sigma) was added to the polymer solution, resulting in a 0.1% w/v final concentration.

Hydrogel films were created using by photocrosslinking the polymer solution in a chamber consisting of a Teflon™ base, silicone spacer (250 μm thickness with 27 mm circle punched out), and a 34 mm circular glass coverslip treated with 3-(Trimethoxysilyl) propyl methacrylate to have methacrylate groups exposed for covalently binding the hydrogel film (46). The peptide-PEGDA solution was placed inside the chamber and exposed to 365 nm UV light (10 mW/cm^2) through the glass for 45 s to cross-link the hydrogel. The 34 mm glass coverslips with covalently bound hydrogel films were then transferred to 6-well plates for further experimentation. 0.25×10^6 freshly isolated hepatocytes or hepatocytes released from culture in double collagen gel, Matrigel, or coculture with fibroblasts were seeded onto hydrogel films in the absence of serum and incubated at 37°C for 6 h. The substrates were then washed twice with PBS to remove nonadherent cells. Cells in six fields per well and three wells per condition were counted using light microscopy.

Hydrogel chemistry and photopatterning

PEGDA (3400 MW, Nektar Therapeutics, Huntsville, AL, USA) was dissolved in PBS at 40% w/v to form a 2× prepolymer solution. Acryloyl-PEG-RGDS (52) was combined with the prepolymer solution to achieve a 40 μmol/mL concentration of RGDS in the 2× solution. 2-hydroxy-1-[4-(2-hydroxyethoxy)phenyl]-2-methyl-1-propanone (Irgacure 2959, Ciba Specialty Chemicals, Tarrytown, NY, USA) was dissolved in 1-vinyl-2-pyrolidone (100 mg/mL) (Sigma) to form the photoinitiator stock solution, and this solution was added to the prepolymer solution to form 0.2% w/v of initiator. Cells suspended in medium were added to prepolymer solution in a 1:1 vol ratio, resulting in a final prepolymer solution containing 5–15 million/mL hepatocytes, 20 μmol/mL RGDS, 20% w/v PEGDA, and 0.1% w/v photoinitiator.

Patterning of the hydrogel was achieved using the apparatus described in previously (46). Clean 34 mm cover glass circles (Fisher Scientific) were treated with a 2% v/v solution of 3-(trimethoxysilyl) propyl methacrylate (Aldrich, Milwaukee, WI, USA) in 95% ethanol (pH 5 with acetic acid) for 2

min, rinsed with 100% ethanol, and then baked at 100°C for at least 5 min to create free methacrylate groups on the glass. The hydrogel solution was sandwiched between the glass and the Teflon™, with the height of the chamber determined by the thickness of the silicone spacer used. An emulsion mask (designed using Corel Draw 11.0 and printed using a commercial Linotronic-Hercules 3300 dpi high-resolution line printer) was placed against the glass circle and chamber was exposed to 100 mW/cm^2 of 365 nm UV light (as measured before passing through the glass slides and mask; 64 mW/cm^2 of light passes through the glass and emulsion mask layers to reach the polymer solution) for 90–110 s using an EXFO Lite UV spot curing system equipped with a 365 nm light filter and a collimating lens (EXFO, Mississuaga, ON, Canada). Addition of layers was accomplished by washing the uncrosslinked solution with PBS and repeating the process using a thicker spacer and new mask. Crosshairs were included as markers on the masks and glass wafers to allow for alignment of successive layers. After completion of patterning, the hydrogel containing cells was washed with PBS and placed in a Petri dish containing culture medium. Alternatively, hydrogels were also fabricated as one thick layer using a mask with no internal pattern to create "bulk" hydrogel constructs for comparison studies.

Bioreactor design

A perfusion circuit, designed and assembled as described previously (53), provided a constant supply of nutrients to the hepatic constructs. Hepatic constructs were perfused in a bioreactor chamber consisting of a simple flow-through chamber with a stainless steel porous platen to support the sample while allowing perfusion through the chamber (54). Flow circuits were set up in parallel so that two separate bioreactor chambers could be perfused simultaneously. Negative pressure-driven flow was continuous (0.5 ml/min) using a programmable push-pull syringe pump (Harvard Apparatus, Holliston, MA, USA). Culture medium drawn from the reservoir was equilibrated with 5% carbon dioxide and air balance in a gas exchanger made with gas-permeable silastic tubing before entering the perfusion chambers. All circuit components except for the syringe pump were housed in a PID-controlled incubator maintained at 37°C. The tubing and connectors were sterilized by autoclave prior to use.

Hepatocyte viability and function

Cell viability was visualized qualitatively using the MTT assay, in which the tetrazolium ring of the MTT (3-(4,5-dimethylthiazol-2-yl)-2,5-diphenyl tetrazolium bromide; Sigma) is cleaved by mitochondrial dehydrogenase enzymes of living cells to form a purple precipitate. The hydrogels containing cells were incubated for 3 h with a 0.5 mg/mL solution of MTT in DMEM without phenol red. Cells that have formed the precipitate appear dark purple under light microscopy.

Albumin synthesis, a surrogate marker of protein synthesis for hepatocytes, was used to measure the function of the hepatocytes within hydrogels. Samples of culture medium were collected and assayed for bulk albumin using an HRP-TMB ELISA assay (Ultra-TMB-S, Research Diagnostics, Flanders, NJ, USA). An intracellular albumin Ab assay was used to visualize the albumin within the hydrogels (55). Urea synthesis was also measured as a marker of liver specific function using a protocol previously described (55).

Microscopy and digital volumetric imaging

Hydrogels and cells were observed and recorded using a Nikon TE300 inverted microscope and digital camera (Photometrics CoolSnap HQ; Roper Scientific, Tucson, AZ, USA) capable of epifluorescence and Hoffman modulation contrast microscopy along with the MetaMorph Image Analysis System (Universal Imaging, Westchester, PA, USA). Alternatively, color photos were taken with a Nikon CoolPix 4300 digital camera that could attach to the microscope. Laser scanning confocal microscopy (Bio-Rad MRC-1024UV, Hercules, CA, USA) was used to image hydrogels containing fluorescently labeled cells.

For digital volumetric imaging (DVI; ref. 56), samples were fixed in 0.5% gluteraldehyde at room temperature for 30 min, embedded in resin (Nanoblast Miniset Embedding Kit, Polysciences, Warrington, PA, USA) with black India ink opacifier (Higgins), and imaged at 4× magnification. Images were visualized using RESView 3.0 software (Microscience Group, Inc., Corte Madera, CA, USA) as 3D renderings, and exported into Matlab 7.0 software (The Mathworks Inc., Natick, MA, USA) to create image rotations.

Statistics and data analysis

Error bars represent SD, with $n = 3$ for toxicity, matrix adhesion, and peptide-film adhesion experiments. Bioreactor experiments allowed duplicates of hydrogel perfusion in each of the two runs. Statistical significance was determined using one-way ANOVA followed by Tukey's Multiple Comparison Test. Unless otherwise stated, statistical significance was determined with $P < 0.05$. The flow cytometry experiments were repeated twice, and the results presented were collected from one full experiment, with trends representative of all experiments.

RESULTS AND DISCUSSION

Overview

Figure 1 schematically depicts the fabrication method developed in this study for additive photopatterning of 3D tissue constructs. We specifically apply this technique to the fabrication of hepatic tissue constructs by tailoring both hydrogel chemistry and architecture. Hepatocytes are fragile, adhesion-dependent cells; therefore, we also developed methods to stabilize cells after isolation and ligate cell surface integrins in order to promote survival and retention of liver-specific functions over two weeks (Supplemental Fig. 1). To explore the capability of the technique, we photopattern both single-layer hydrogel structures that reduce nutrient transport limitations and multilayer constructs with fluidic channels that enable perfusion in a continuous-flow bioreactor. 3D hepatic tissues were characterized by digital volumetric imaging and by monitoring albumin and urea synthesis as markers of liver-specific function.

Hepatocyte integrin expression and adhesion to extracellular matrix

To address the issue of tailoring PEG hydrogels for hepatocytes by incorporating adhesion peptides, we

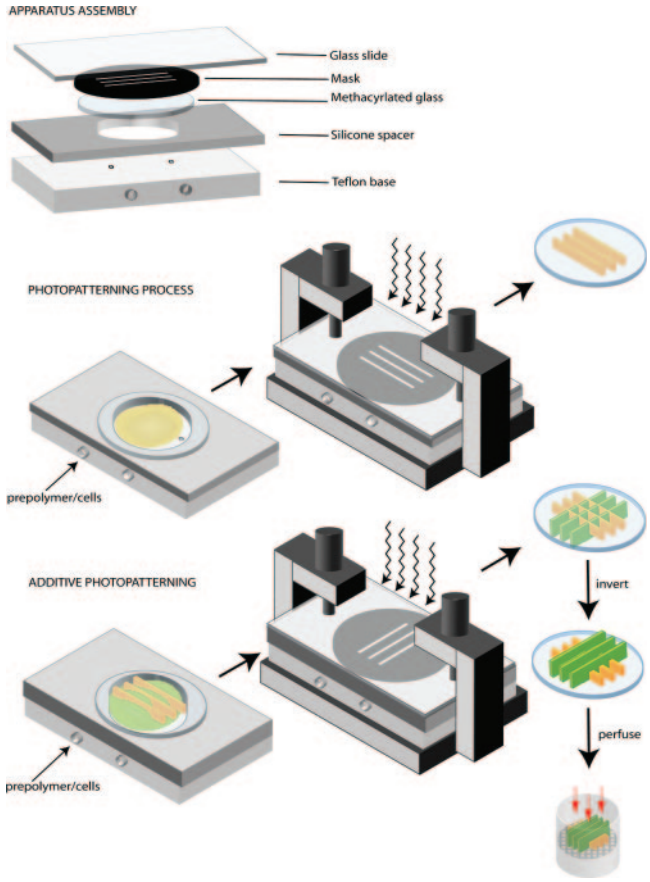

Figure 1. Fabrication of living tissues by additive photopatterning of cellular hydrogels. Schematic depiction of fabrication process indicates enclosed chamber, filled with cell-laden prepolymer solution, and exposure to light through a photomask causes photocrosslinking in pattern with microscale features. The height of the chamber is then increased and the process repeated, resulting in a multilayer cell-laden tissue construct with microscale features. Controlled scaffold architecture enables convective transport on perfusion.

probed the integrin expression profile of hepatocytes to better understand the types of adhesive ligands that may be effective. In addition to examining freshly isolated hepatocytes, we were also interested in changes that occur in integrin expression under various cell culture models that would be used to stabilize the cells prior to encapsulation. Flow cytometry was used to determine the integrin expression profile of primary hepatocytes that were freshly isolated or cultured for up to one week. Results for freshly isolated hepatocytes indicated that α_1, α_5, and β_1 were expressed on the cell surface (data not shown). α_3 and α_6 integrin subunits were barely detectable under these experimental conditions. The subunits α_2 and α_4 were not expressed by freshly isolated rat hepatocytes.

The shifts of the arithmetic means are plotted for integrin subunits α_1, α_3, α_5, and integrin $\alpha_6\beta_1$ in Supplemental Fig. 2 to compare the expression of hepatocytes that were freshly isolated and those that had been cultured in coculture with fibroblasts, in a collagen double gel sandwich configuration, and on Matrigel over a period of a week (all three methods have been described to stabilize the phenotype of hepatocytes *in vitro*). Results indicated that α_1 integrin subunit expression was maintained across culture conditions, whereas changes in expression level were observed for subunit α_5 and integrin $\alpha_6\beta_1$. Although α_5 was detected in freshly isolated hepatocytes, the expression level declines in cultured cells within the first day. Hepatocytes cocultured with fibroblasts could recover their α_5 subunit expression with time, while those cultured in double gel maintained the lowered expression level and Matrigel cultures experienced a further decline. The up-regulation of integrin expression on cocultured cells may be a result of the presence of fibronectin, associated with $\alpha_5\beta_1$, which is produced by fibroblasts. Conversely, hepatocytes that were cultured on Matrigel, a matrix composed mostly of laminin, continued to lose expression of the α_5 integrin subunit over 7 d. This may be explained by the fact that hepatocytes cultured on Matrigel form spheroids, resulting in increased cell-cell interactions and decreased cell-matrix interactions. Surprisingly, the levels of $\alpha_6\beta_1$ integrin increased in cultured cells, even though expression was barely detectable in freshly isolated cells. Notably, although $\alpha_6\beta_1$ is not typically found in healthy adult liver, hepatocytes have been reported to upregulate expression of both this integrin and laminin production in some disease states (57).

Based on the flow cytometry results, we hypothesized that hepatocytes stabilized in culture might be altered in their capacity to adhere to full-length ECM or their adhesive peptides. Adhesion of hepatocytes on fibronectin, collagen I, laminin, and vitronectin were therefore evaluated (Supplemental Fig. 3). After incubation for 4 h in the absence of serum, freshly isolated hepatocytes attached and spread to fibronectin, collagen, and laminin substrates, but did not adhere to vitronectin. Hepatocytes that had been cultured on Matrigel, in contrast, were not able to adhere to matrix substrates to any large degree. Hepatocytes released from collagen gel could attach to matrix, and some cell spreading was observed. The levels of integrin expression as compared among various culture conditions after 7 d was consistent with their ability to adhere to matrix substrates: coculture > double gel > Matrigel for all conditions. The flow cytometry results for α_1, α_5, and $\alpha_6\beta_1$ all yielded similar results when comparing different culture conditions: cocultured hepatocytes expressed the highest levels of integrins, cells cultured on Matrigel expressed the lowest levels, and double gel cultured cells expressed medium levels of integrins (higher than Matrigel, lower than coculture). Therefore, these semiquantitative results indicate that cocultivation with fibroblasts may serve the dual purpose of inducing liver-specific functions and preserving maximal levels of functional integrin expression. This indicates that stabilization of hepatocytes in coculture may better prepare the cells for incorporation into biomaterials by increasing their affinity to ligands as compared to other culture models.

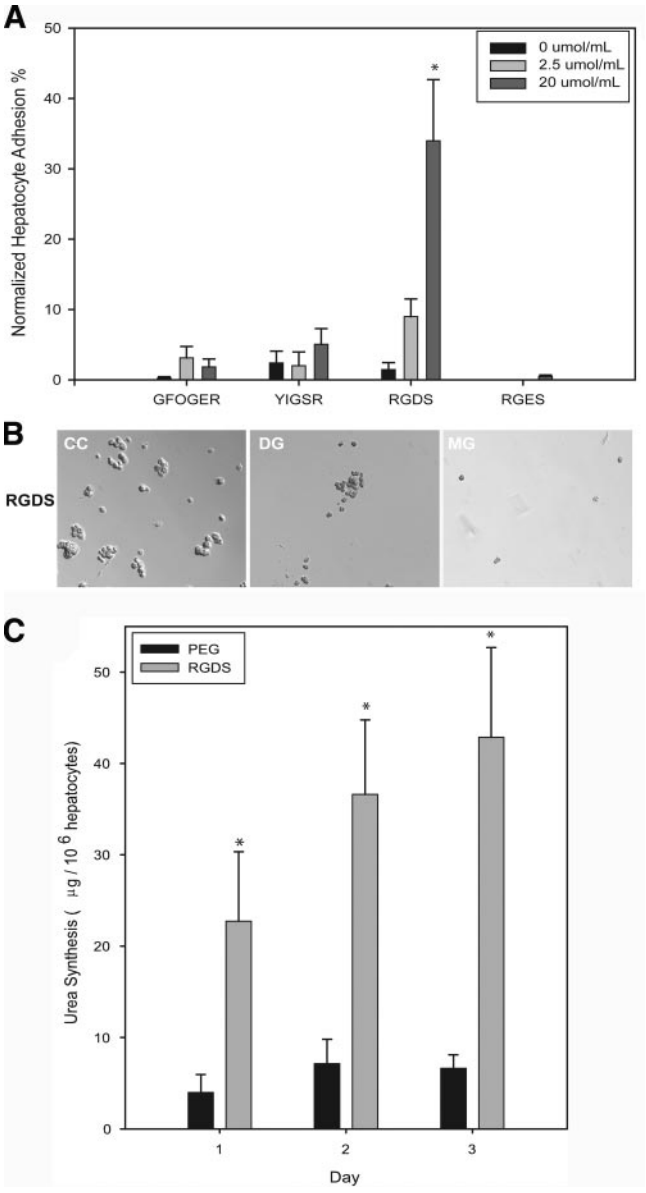

Figure 2. Tailoring hydrogel chemistry and hepatocyte culture conditions to promote cell survival in PEG hydrogels. *A)* Adhesion of freshly isolated hepatocytes on PEG thin films doped with adhesion peptides GFOGER, YIGSR, RGDS selected from collagen, laminin, and fibronectin to ligate hepatocyte integrins (Supplemental Fig. 2). RGES is a negative control. Maximal adhesion is observed on 20 μmol/mL RGDS films. Adhesion is expressed relative to the number of cells that adhere to an equal surface area of collagen-coated tissue culture polystyrene (normalized hepatocyte adhesion %) and data are mean ± SD (n=3). Since freshly isolated hepatocytes do not survive photopolymerization in PEG hydrogels but survival is improved on 1 wk of cell culture to recover from isolation (Supplemental Fig. 1), the influence of culture conditions on integrin expression and matrix adhesion were investigated (Supplemental Fig. 3). *B)* Adhesion of cultured hepatocytes on 20 μmol/mL RGDS thin film varies with culture condition: cocultivation with stromal cells (CC), culture between two layers of collagen gel (double gel, DG), and matrigel (MG) each for 7 d. Maximal adhesion is observed on RGDS films after cocultivation. Data are mean ± SD (n=3). The (*) denotes statistical difference (P<0.05) between RGDS 20 umol/mL and 0 umol/mL conditions (One-way ANOVA, Tukey's Multiple Comparison Test). *C)* Hepatocytes are cocultured for 1 wk and then encapsulated in 20 μmol/mL RGDS. Liver-specific function, as indicated by urea production, is improved over PEG alone. Data are mean ± SD (n=3). The (*) denotes statistical difference (P<0.05) between PEG and RGDS conditions (One-way ANOVA, Tukey's Multiple Comparison Test).

Hepatocyte adhesion on peptide films

Next, we embarked on studies to translate insights from cell adhesion to full length ECM to selection of synthetic peptides to incorporate into inert PEG hydrogels to improve hepatocyte viability and function. The use of small peptides for promoting interaction with biomaterials is desirable because they are relatively stable compared with whole matrix molecules, are easily conjugated to biomaterials, are easily synthesized, and have low immunogenic activity (58). The peptides studied included RGDS (Arg-Gly-Asp-Ser, derived from fibronectin), YIGSR (Tyr-Ile-Gly-Ser-Arg, derived from laminin), GF-(Hyp)GER (Gly-Phe-HydroxyPro-Gly-Glu-Arg, derived from collagen), KQAGDV (Lys-Gln-Ala-Gly-Asp-Val, derived from fibrinogen), and the negative control RGES (Arg-Gly-Glu-Ser). Peptides were incorporated into PEGDA hydrogel films, and adhesion on these surfaces was compared to adhesion on PEGDA only gels (negative control) as well as adsorbed collagen I (positive control).

Adhesion of freshly isolated and precultured hepatocytes was investigated. Overall, adhesion of freshly isolated hepatocytes was minimal for peptide-doped hydrogels as compared to adhesion on adsorbed ECM. Hepatocytes did not spread appreciably on any of the PEG-peptide films. In contrast, fibroblasts seeded on RGDS films attached and spread in a dose-dependent manner (not shown), verifying that the peptides were indeed present and available for binding. Of the peptides used in this study, only RGDS was able to confer hepatocyte adhesion but not spreading for the concentrations tested, similar to previous reports (**Fig. 2*A***) (59–62). A negative control of a similar peptide, RGES, was also examined to rule out the non-specific binding to the short peptide.

Hepatocytes cultured in double collagen gel, on Matrigel, and in coculture with fibroblasts for 1 wk were seeded onto 20 μmol/mL RGDS-doped PEGDA films to determine adhesion capabilities of precultured hepatocytes. Results were similar to those on full-length ECM in that cells that had been cultured on Matrigel demonstrated the least adhesion to RGDS-PEG films, while those that had been cocultured with fibroblasts demonstrated the highest levels of adhesion (Fig. 2*B*). Based on these results, a combination of coculture of hepatocytes with fibroblasts followed by incorporation into a PEG hydrogel containing 20 μmol/mL of RGDS were used as a starting point for fabrication of a hepatic construct.

Hepatocyte adhesion to YIGSR has been shown previously when grafted onto polymer surfaces (63), but we were unable to demonstrate attachment in the range of

peptide concentrations tested. Although hepatocytes did not spread on RGD-containing surfaces, it has been shown previously that rounded cells on matrix surfaces (low density) preserve liver-specific function, while hepatocytes that spread on high-density matrix substrates lose phenotypic stability over time (61, 62). The incorporation of RGD peptides in gels with hepatocytes is not unprecedented—hepatocyte spheroids cultured in thermoreversible gels containing RGD have been reported to maintain viability and liver-specific functionality at a higher level than in the same biomaterial without RGD peptides (64). In addition, transformed, SV-40 immortilized murine hepatocytes exhibit enhanced albumin production when cultured in PEG hydrogels incorporating RGD peptides compared to PEG hydrogels without peptide (65).

A lack of adhesion in our peptide-doped hydrogel adhesion study is not an absolute indicator that hepatocytes cannot adhere to these peptides; integrin binding to peptides may be affected by the way in which the peptides are presented (adjacent amino acids, spacer chains, concentration of peptides for clustering, synergy domains, *etc.*). It has been reported that integrin binding to RGD requires a PHSRN synergy domain (66). While groups have shown that the PHSRN synergy site is unnecessary for $\alpha_5\beta_1$ integrin that is in the activated state (67, 68), Garcia and coworkers have maintained that synergy plays a role in cell adhesion to RGD (69, 70). Alternatively, others have shown that the affinity of cell binding can be modulated by varying the presentation of RGD from various tether lengths (71, 72) or in nanoscale clusters (40, 73). A combination of peptides may also provide a more effective approach to cell adhesion (74). It has also been suggested that incorporation of protein domains may enhance adhesion as compared to the minimalist peptide sequences because they retain more characteristics of the natural matrix molecules (75). Other, carbohydrate-based domains may also improve on hepatocyte adhesion. For example, incorporation of galactose-derived sugars onto various surfaces have been reported to confer hepatocyte adhesion and spreading via an asialoglycoprotein receptor (76–78), and may offer an alternative to or work in conjunction with adhesion peptides. Finally, it is also possible to incorporate certain whole matrix molecules such as fibronectin into biomaterials to achieve cell attachment (79–81).

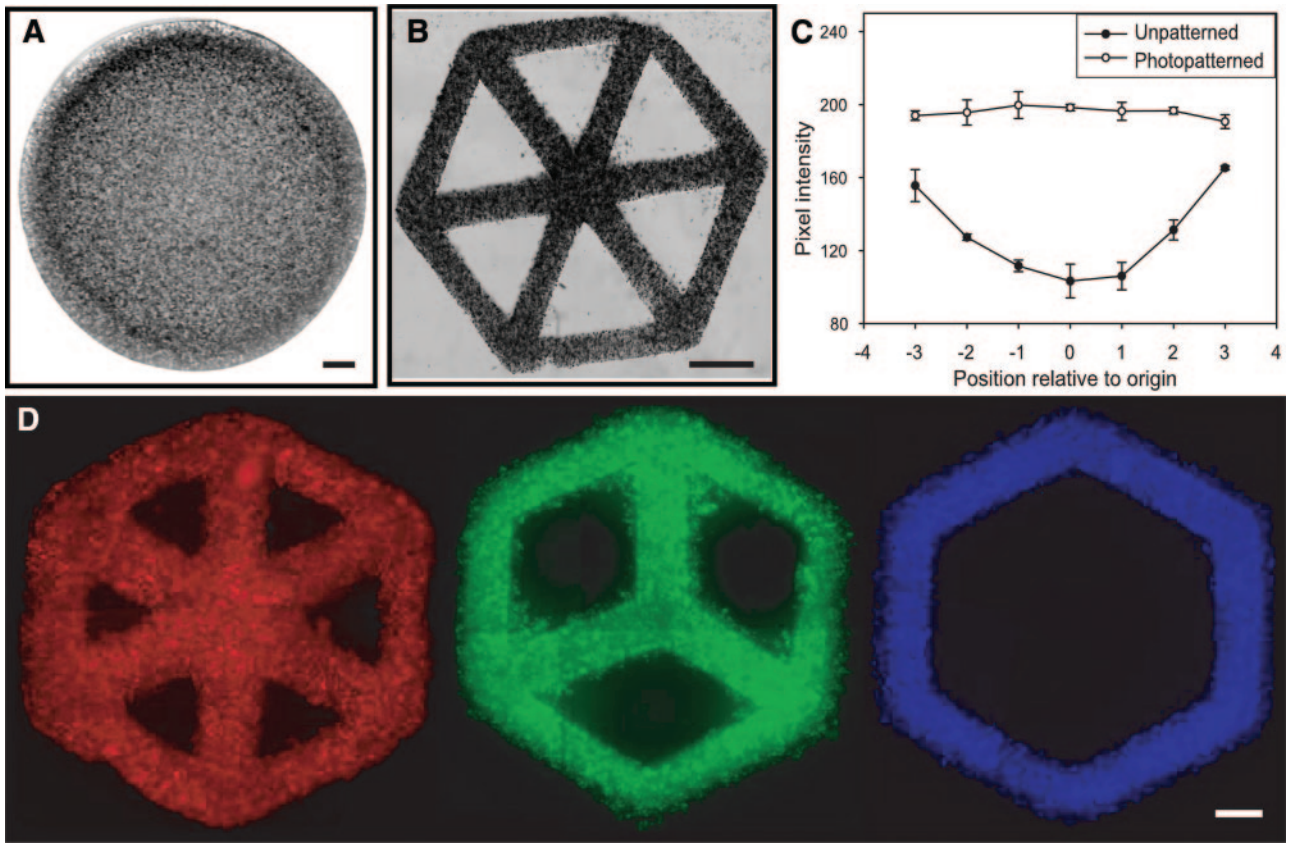

Figure 3. Photopatterning of hepatocytes in a single layer improves diffusive nutrient transport and viability. *A)* Hepatocytes at 7.5×10^6 cells/ml density encapsulated in hydrogel plug 1.5 mm thick and 10 mm diameter. Viability indicated by black MTT stain for mitochondrial activity. Central pallor indicates necrotic core due to transport limitations. Scale bar is 500 μm. *B)* Hepatocytes at same density and macroscopic hydrogel dimensions in (*A*), with photopatterned features of 500 μm, thereby reducing diffusive transport barrier. Scale bar is 1 mm. *C)* Quantitation of OD in photomicrographs. The reduction of OD by ~55% in the core *vs.* edge of the unpatterned hydrogel plug (closed circles) is mitigated by photopatterning (open circles). Mean OD ± SD of a representative construct is shown (n=3). *D)* Versatility in photopatterning is demonstrated by multiple microscale patterns. Viable cells are labeled with fluorescent dyes CMTMR (red), CMFDA (green) and CMAC (blue). Scale bar is 500 μm.

Hepatocytes encapsulated in RGD-doped PEG hydrogels

Based on the results described above, hepatocytes were stabilized in coculture after isolation and then photoencapsulated into RGDS-doped PEG hydrogel discs. The incorporation of 20 μmol/mL RGDS increased the liver-specific function by 5-fold over PEG controls over 3 days, as assessed by urea secretion (Fig. 2*C*) and albumin production (not shown).

Next, we investigated the potential for photopatterning of the hydrogels to improve nutrient transport and hepatocyte viability in single layer constructs by assessing mitochondrial activity by MTT 24 h after photoencapsulation (**Fig. 3**). Hepatocytes were photoencapsulated at density of 7.5×10^6 cells/ml in hydrogel discs of 1.5 mm thickness and 10 mm diameter and compared to constructs of the same density and outer dimensions (1.5 mm thickness, 10 mm diameter) but with photopatterned features of 500 μm. Hydrogel discs exhibited central pallor in MTT staining consistent with a necrotic core, whereas photopatterned constructs retained dark staining throughout the construct (Figs. 3*A*, *B*). Densitometry analysis of photomicrographs revealed that the ~55% reduction of optical density (OD) in the core *vs.* edge of the unpatterned hydrogel plug is mitigated by photopatterning (Fig. 3*C*). Thus, photopatterning of hydrogels facilitates the transport of oxygen and nutrients required to meet the high metabolic demands of encapsulated hepatocytes.

Using the parameters identified for homogenous MTT staining in photopatterned constructs, three single-layer patterns were constructed and viability was confirmed by loading with fluorescent membrane integrity dyes (Fig. 3*D*). These data set the stage for fabrication of multilayer constructs by assembling the individual layers.

Multilayer 3D hepatic tissue construct

The design of the multilayer hepatic construct consisted of a three-layered hexagonal branching structure that served to demonstrate the utility of the photopatterning technology, minimize transport limitations, and mimic the branching architecture of the liver *in vivo*. The patterning masks utilized to generate this

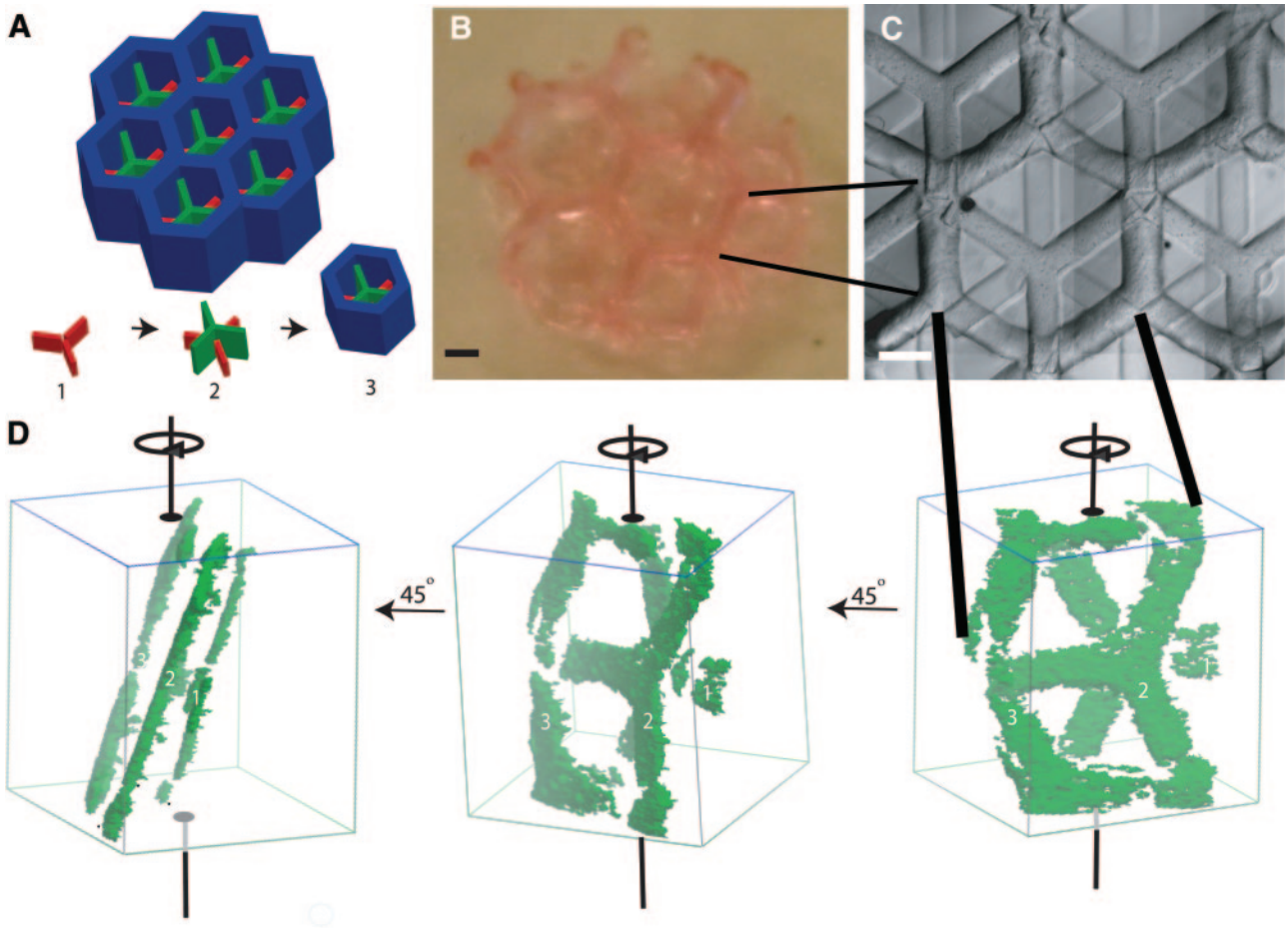

Figure 4. Additive photopatterning of cellular hydrogels to fabricate tissue with 3D microarchitecture. *A)* Design of photopattern for each layer: red (1), green (2), and blue (3). *B)* Photograph of resultant 3D microscale hepatic tissue. Scale bar is 1 mm. *C)* Phase contrast micrograph of three-layer tissue. Scale bar is 500 μm. *D)* 3D reconstruction from sequential histological sections of three-layer tissue with fluorescently labeled cells (and supplementary video). Details on digital volumetric imaging are described in Materials and Methods.

construct were designed to provide single UV exposures to all regions of cells despite the need for three photopatterning steps (**Fig. 4*A***). Fluorescently labeled hepatocytes were incorporated into the hydrogel fabrication process for visualization by digital volumetric imaging (Fig. 4*B–D*). The 3D rendering (Supplemental Movie) demonstrates the incorporation of cells in three clearly identifiable layers of the tissue construct.

Scale-up without transport limitations represents a challenging issue in hepatic tissue engineering, as hepatocytes are highly metabolic and require a nearby nutrient supply source for viability and phenotypic stability (82, 83). Therefore, to evaluate the liver-specific function of the multilayer construct, the tissue was transferred to a perfusion bioreactor. The channels created in the multilayer structure allow for convective flow of culture medium through the construct and relatively short distance for diffusive transport to all encapsulated cells. After 1 or 3 d in the bioreactor, samples were removed and again imaged using MTT as a marker of metabolic activity. **Figure 5** depicts hydrogel constructs from days 1 and 3, demonstrating that viable cells are visible throughout all three layers of the construct. Culture medium collected over 12 d in perfusion culture was assayed for albumin and urea synthesis, which serve as representative markers of synthetic and metabolic function in the liver. Hepatic constructs cultured in the bioreactor produced higher levels of both albumin and urea than unpatterned constructs of equal cell number and external scaffold dimensions (Fig. 5*D, E*). The levels of albumin production are comparable with those reported for hepatocyte spheroids in rotating cultures (84) but are lower than albumin produced by hepatocytes stabilized in 2D coculture (55). Urea synthesis, however, is on par with levels measured in stabilized 2D cultures (55). The levels of function achieved in the patterned, perfused constructs can be attributed to the deliberate incorporation of a combination of microenvironmental factors, including cell-cell interactions, adhesive peptides and improved nutrient transport. Hydrogels can also be tailored to incorporate additional bioactive ligands (85, 86), degradable linkages (87, 88), pore sizes that promote protein release (89) or other supporting cell types (*e.g.*, endothelial cells) organized in defined layers. Strategic manipulation and optimization of these parameters promises to allow further enhancement of hepatocyte functions. Collectively, our results indicate that 3D hepatic tissue constructs can be fabricated using multilayer photopatterning and maintained for two weeks in a perfusion bioreactor, setting the stage for further *in vitro* and *in vivo* studies.

CONCLUSIONS

The fabrication of a functional 3D hepatic construct with a complex internal architecture has been demonstrated. In the future, we propose that the fabrication of 3D cell-laden hydrogels by additive photopatterning can be easily generalized to many tissue types. Use of a widely utilized photopolymerizable biomaterial such as PEGDA enables the straightforward incorporation of tethered biomolecules (adhesive ligands, cytokines) and modification of pore size and degradation rates that may be required by other cell and tissue types. Use

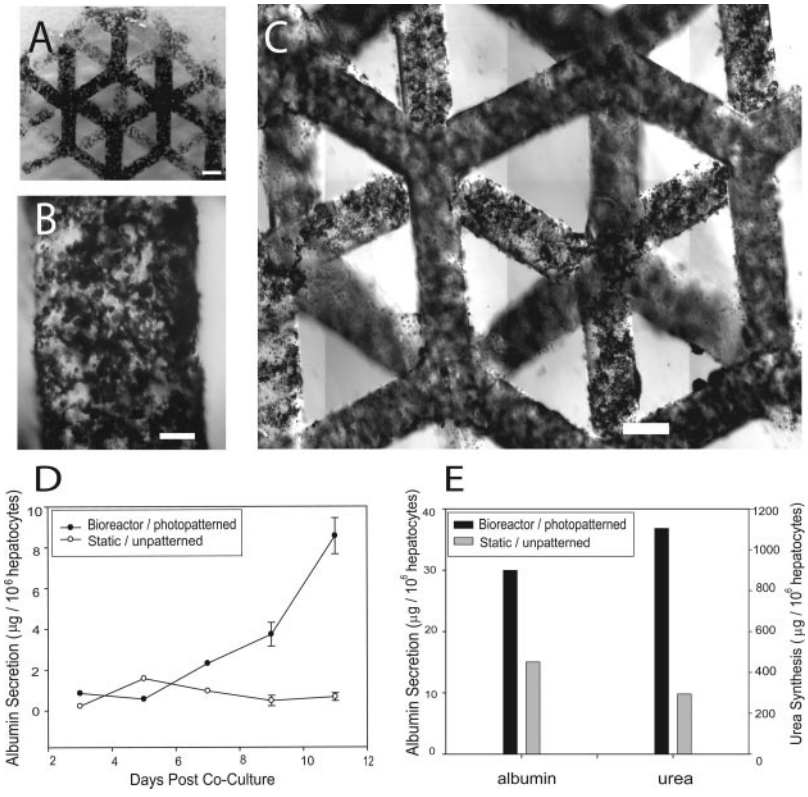

Figure 5. Viability and Function of perfused microscale hepatic tissue. Three-layer constructs visualized in Fig. 4 were perfused in a continuous flow bioreactor and stained for viability. *A)* Low-magnification photomicrograph of black MTT stain in multilayer hepatic construct after 1 d of perfusion. Scale bar is 500 μm. *B)* High-magnification photomicrograph of a single strut after 3 d of perfusion indicates viable cells throughout the tissue. Scale bar is 100 μm. *C)* High-magnification photomicrograph of 1 d perfused construct enables visualization of viable cells in all three layers. Scale bar is 500 μm (*D*) Liver-specific function, as measured by albumin secretion, of perfused microscale hepatic tissue as compared to unperfused plug of the same cell density and macroscopic dimensions. Error bars represent SD of the mean (n=3). *E)* Comparison of cumulative albumin secretion and urea synthesis between perfused, microscale tissue and unperfused plug indicate 100–260% improvements in hepatic function.

of a multilayer process enables the incorporation of different cell types in each layer which may be required for some applications (90). Therefore, use of multilayer photopatterning to further specify microscale tissue architecture enables progress toward the goal of so-called "organ printing". From a fundamental perspective, combining multilayer photopatterning with techniques to organize cells within hydrogels will allow investigation of structure/function relationships in a 3D tissue context (91, 92). FJ

We thank Gregory Underhill for advice on flow cytometry and Jennifer Felix and Kathryn Hudson for hepatocyte isolation. These studies were funded, in part, by the Whitaker Foundation (V.L.T.), the American Association of University Women (V.L.T.), Achievement Rewards for College Scientists (V.L.T.), NSF CAREER (S.N.B), NIH NIDDK, the David and Lucile Packard Foundation, and NASA.

REFERENCES

1. Demetriou, A. A., Whiting, J. F., Feldman, D., Levenson, S. M., Chowdhury, N. R., Moscioni, A. D., Kram, M., and Chowdhury, J. R. (1986) Replacement of liver function in rats by transplantation of microcarrier-attached hepatocytes. *Science* **233,** 1190–1192
2. Hamazaki, K., Doi, Y., and Koide, N. (2002) Microencapsulated multicellular spheroid of rat hepatocytes transplanted intraperitoneally after 90% hepatectomy. *Hepatogastroenterology* **49,** 1514–1516
3. Dixit, V., Darvasi, R., Arthur, M., Brezina, M., Lewin, K., and Gitnick, G. (1990) Restoration of liver function in Gunn rats without immunosuppression using transplanted microencapsulated hepatocytes. *Hepatology* **12,** 1342–1349
4. Mooney, D. J., Sano, K., Kaufmann, P. M., Majahod, K., Schloo, B., Vacanti, J. P., and Langer, R. (1997) Long-term engraftment of hepatocytes transplanted on biodegradable polymer sponges. *J. Biomed. Mater. Res.* **37,** 413–420
5. Vacanti, J. P., Morse, M. A., Saltzman, W. M., Domb, A. J., Perez-Atayde, A., and Langer, R. (1988) Selective cell transplantation using bioabsorbable artificial polymers as matrices. *J. Pediat. Surg.* **23,** 3–9
6. Dvir-Ginzberg, M., Gamlieli-Bonshtein, I., Agbaria, R., and Cohen, S. (2003) Liver tissue engineering within alginate scaffolds: effects of cell-seeding density on hepatocyte viability, morphology, and function. *Tissue. Eng.* **9,** 757–766
7. Davis, M. W. and Vacanti, J. P. (1996) Toward development of an implantable tissue engineered liver. *Biomaterials* **17,** 365–372
8. Takezawa, T., Inoue, M., Aoki, S., Sekiguchi, M., Wada, K., Anazawa, H., and Hanai, N. (2000) Concept for organ engineering: a reconstruction method of rat liver for in vitro culture. *Tissue Eng.* **6,** 641–650
9. Kim, S. S., Sundback, C. A., Kaihara, S., Benvenuto, M. S., Kim, B. S., Mooney, D. J., and Vacanti, J. P. (2000) Dynamic seeding and in vitro culture of hepatocytes in a flow perfusion system. *Tissue Eng.* **6,** 39–44
10. Kaihara, S., Kim, S., Kim, B. S., Mooney, D. J., Tanaka, K., and Vacanti, J. P. (2000) Survival and function of rat hepatocytes cocultured with nonparenchymal cells or sinusoidal endothelial cells on biodegradable polymers under flow conditions. *J. Pediatr. Surg.* **35,** 1287–1290
11. Kaihara, S., Borenstein, J., Koka, R., Lalan, S., Ochoa, E. R., Ravens, M., Pien, H., Cunningham, B., and Vacanti, J. P. (2000) Silicon micromachining to tissue engineer branched vascular channels for liver fabrication. *Tissue Eng.* **6,** 105–117
12. Hasirci, V., Berthiaume, F., Bondre, S. P., Gresser, J. D., Trantolo, D. J., Toner, M., and Wise, D. L. (2001) Expression of liver-specific functions by rat hepatocytes seeded in treated poly(lactic-co-glycolic) acid biodegradable foams. *Tissue Eng.* **7,** 385–394
13. Lee, H., Cusick, R. A., Browne, F., Ho Kim, T., Ma, P. X., Utsunomiya, H., Langer, R., and Vacanti, J. P. (2002) Local delivery of basic fibroblast growth factor increases both angiogenesis and engraftment of hepatocytes in tissue-engineered polymer devices. *Transplantation* **73,** 1589–1593
14. Uyama, S., Kaufmann, P. M., Kneser, U., Fiegel, H. C., Pollok, J. M., Kluth, D., Vacanti, J. P., and Rogiers, X. (2001) Hepatocyte transplantation using biodegradable matrices in ascorbic acid-deficient rats: comparison with heterotopically transplanted liver grafts. *Transplantation* **71,** 1226–1231
15. Sun, W. and Lal, P. (2002) Recent development on computer aided tissue engineering—a review. *Comput. Methods Programs. Biomed.* **67,** 85–103
16. Sachlos, E., Reis, N., Ainsley, C., Derby, B., and Czernuszka, J. T. (2003) Novel collagen scaffolds with predefined internal morphology made by solid freeform fabrication. *Biomaterials* **24,** 1487–1497
17. Griffith, L. G. (2002) Emerging design principles in biomaterials and scaffolds for tissue engineering. *Ann. N. Y. Acad. Sci.* **961,** 83–95
18. Taboas, J. M., Maddox, R. D., Krebsbach, P. H., and Hollister, S. J. (2003) Indirect solid free form fabrication of local and global porous, biomimetic and composite 3D polymer-ceramic scaffolds. *Biomaterials* **24,** 181–194
19. Leong, K. F., Cheah, C. M., and Chua, C. K. (2003) Solid freeform fabrication of three-dimensional scaffolds for engineering replacement tissues and organs. *Biomaterials* **24,** 2363–2378
20. Cooke, M. N., Fisher, J. P., Dean, D., Rimnac, C., and Mikos, A. G. (2003) Use of stereolithography to manufacture critical-sized 3D biodegradable scaffolds for bone ingrowth. *J. Biomed. Mater. Res.* **64B,** 65–69
21. Zein, I., Hutmacher, D. W., Tan, K. C., and Teoh, S. H. (2002) Fused deposition modeling of novel scaffold architectures for tissue engineering applications. *Biomaterials* **23,** 1169–1185
22. Sodian, R., Loebe, M., Hein, A., Martin, D. P., Hoerstrup, S. P., Potapov, E. V., Hausmann, H., Lueth, T., and Hetzer, R. (2002) Application of stereolithography for scaffold fabrication for tissue engineered heart valves. *Asaio. J.* **48,** 12–16
23. Hutmacher, D. W. (2001) Scaffold design and fabrication technologies for engineering tissues– state of the art and future perspectives. *J. Biomater. Sci. Polym. Ed.* **12,** 107–124
24. Nishimura, I., Garrell, R. L., Hedrick, M., Iida, K., Osher, S., and Wu, B. (2003) Precursor tissue analogs as a tissue-engineering strategy. *Tissue. Eng.* **9 Suppl. 1,** S77–S89
25. Boland, T., Mironov, V., Gutowska, A., Roth, E. A., and Markwald, R. R. (2003) Cell and organ printing 2: fusion of cell aggregates in three-dimensional gels. *Anat. Rec.* **272A,** 497–502
26. Jakab, K., Neagu, A., Mironov, V., Markwald, R. R., and Forgacs, G. (2004) Engineering biological structures of prescribed shape using self-assembling multicellular systems. *Proc. Natl. Acad. Sci. U. S. A.* **101,** 2864–2869
27. Peppas, N. A., Bures, P., Leobandung, W., and Ichikawa, H. (2000) Hydrogels in pharmaceutical formulations. *Eur. J. Pharm. Biopharm.* **50,** 27–46
28. Elisseeff, J., McIntosh, W., Anseth, K., Riley, S., Ragan, P., and Langer, R. (2000) Photoencapsulation of chondrocytes in poly-(ethylene oxide)-based semi-interpenetrating networks. *J. Biomed. Mater. Res.* **51,** 164–171
29. Bryant, S. J. and Anseth, K. S. (2002) Hydrogel properties influence ECM production by chondrocytes photoencapsulated in poly(ethylene glycol) hydrogels. *J. Biomed. Mater. Res.* **59,** 63–72
30. Bryant, S. J. and Anseth, K. S. (2003) Controlling the spatial distribution of ECM components in degradable PEG hydrogels for tissue engineering cartilage. *J. Biomed. Mater. Res.* **64,** 70–79
31. Mann, B. K., Gobin, A. S., Tsai, A. T., Schmedlen, R. H., and West, J. L. (2001) Smooth muscle cell growth in photopolymerized hydrogels with cell adhesive and proteolytically degradable domains: synthetic ECM analogs for tissue engineering. *Biomaterials* **22,** 3045–33051
32. Behravesh, E., Zygourakis, K., and Mikos, A. G. (2003) Adhesion and migration of marrow-derived osteoblasts on injectable in situ crosslinkable poly(propylene fumarate-co-ethylene glycol)-based hydrogels with a covalently linked RGDS peptide. *J. Biomed. Mater. Res.* **65A,** 260–270

33. Mahoney, M. J. and Anseth, K. S. (2006) Three-dimensional growth and function of neural tissue in degradable polyethylene glycol hydrogels. *Biomaterials* **27,** 2265–2274
34. Gobin, A. S. and West, J. L. (2002) Cell migration through defined, synthetic ECM analogs. *FASEB J.* **16,** 751–753
35. Hern, D. L. and Hubbell, J. A. (1998) Incorporation of adhesion peptides into nonadhesive hydrogels useful for tissue resurfacing. *J. Biomed. Mater. Res.* **39,** 266–276
36. Zheng Shu, X., Liu, Y., Palumbo, F. S., Luo, Y., and Prestwich, G. D. (2004) In situ crosslinkable hyaluronan hydrogels for tissue engineering. *Biomaterials* **25,** 1339–1348
37. Alhadlaq, A., Tang, M., and Mao, J. J. (2005) Engineered adipose tissue from human mesenchymal stem cells maintains predefined shape and dimension: implications in soft tissue augmentation and reconstruction. *Tissue. Eng.* **11,** 556–566
38. Hwang, N. S., Kim, M. S., Sampattavanich, S., Baek, J. H., Zhang, Z., and Elisseeff, J. (2006) Effects of three-dimensional culture and growth factors on the chondrogenic differentiation of murine embryonic stem cells. *Stem Cells* **24,** 284–291
39. Kao, W. J. and Hubbell, J. A. (1998) Murine macrophage behavior on peptide-grafted polyethyleneglycol-containing networks. *Bio/Tech. Bioeng.* **59,** 2–9
40. Koo, L. Y., Irvine, D. J., Mayes, A. M., Lauffenburger, D. A., and Griffith, L. G. (2002) Co-regulation of cell adhesion by nanoscale RGD organization and mechanical stimulus. *J. Cell Sci.* **115,** 1423–1433
41. Alsberg, E., Anderson, K. W., Albeiruti, A., Rowley, J. A., and Mooney, D. J. (2002) Engineering growing tissues. *Proc. Natl. Acad. Sci. U. S. A.* **99,** 12025–12030
42. Schmedlen, R. H., Masters, K. S., and West, J. L. (2002) Photocrosslinkable polyvinyl alcohol hydrogels that can be modified with cell adhesion peptides for use in tissue engineering. *Biomaterials* **23,** 4325–4332
43. Sawhney, A. S., Pathak, C. P., van Rensburg, J. J., Dunn, R. C., and Hubbell, J. A. (1994) Optimization of photopolymerized bioerodible hydrogel properties for adhesion prevention. *J. Biomed. Mater. Res.* **28,** 831–838
44. Nuttelman, C. R., Henry, S. M., and Anseth, K. S. (2002) Synthesis and characterization of photocrosslinkable, degradable poly(vinyl alcohol)-based tissue engineering scaffolds. *Biomaterials* **23,** 3617–3626
45. Raeber, G. P., Lutolf, M. P., and Hubbell, J. A. (2005) Molecularly engineered PEG hydrogels: a novel model system for proteolytically mediated cell migration. *Biophys. J.* **89,** 1374–8138
46. Liu, V. A. and Bhatia, S. N. (2002) Three-dimensional photopatterning of hydrogels containing living cells. *Biomed. Microdev.* **4,** 257–266
47. Seglen, P. O. (1976) Preparation of isolated rat liver cells. *Methods Cell Biol.* **13,** 29–83
48. Dunn, J. C., Yarmush, M. L., Koebe, H. G., and Tompkins, R. G. (1989) Hepatocyte function and extracellular matrix geometry: long-term culture in a sandwich configuration [published erratum appears in FASEB J. 1989 May;3(7):1873]. *FASEB J.* **3,** 174–177
49. Dunn, J. C., Tompkins, R. G., and Yarmush, M. L. (1991) Long-term in vitro function of adult hepatocytes in a collagen sandwich configuration. *Biotechnol. Prog.* **7,** 237–245
50. Miyazaki, M., Suzuki, Y., and Sato, J. (1988) A method for rapid preparation of single-cell suspensions from rat hepatocyte primary cultures on collagen substratum and the mechanism of cell dissociation. *Acta Med. Okayama.* **42,** 351–354
51. Ter Brugge, P. J., Torensma, R., De Ruijter, J. E., Figdor, C. G., and Jansen, J. A. (2002) Modulation of integrin expression on rat bone marrow cells by substrates with different surface characteristics. *Tissue. Eng.* **8,** 615–626
52. Mann, B. K., Tsai, A. T., Scott-Burden, T., and West, J. L. (1999) Modification of surfaces with cell adhesion peptides alters extracellular matrix deposition. *Biomaterials* **20,** 2281–2286
53. Allen, J. W. and Bhatia, S. N. (2003) Formation of steady-state oxygen gradients in vitro: application to liver zonation. *Biotechnol. Bioeng.* **82,** 253–262
54. Dunkelman, N. S., Zimber, M. P., Lebaron, R. G., Pavelec, R., Kwan, M., and Purchio, A. F. (1995) Cartilage production by rabbit articular chondrocytes on polyglycolic acid scaffolds in a closed bioreactor system. *Bio/Tech. Bioeng.* **46,** 299–305
55. Bhatia, S. N., Balis, U. J., Yarmush, M. L., and Toner, M. (1998) Probing heterotypic cell interactions: hepatocyte function in microfabricated co-cultures. *J. Biomater. Sci., Polymer Edit.* **9,** 1137–1160
56. Ewald, A. J., McBride, H., Reddington, M., Fraser, S. E., and Kerschmann, R. (2002) Surface imaging microscopy, an automated method for visualizing whole embryo samples in three dimensions at high resolution. *Developmental Dynamics* **225,** 369–375
57. Nejjari, M., Hafdi, Z., Dumortier, J., Bringuier, A. F., Feldmann, G., and Scoazec, J. Y. (1999) alpha6beta1 integrin expression in hepatocarcinoma cells: regulation and role in cell adhesion and migration. *Int. J. Cancer* **83,** 518–525
58. Kantlehner, M., Schaffner, P., Finsinger, D., Meyer, J., Jonczyk, A., Diefenbach, B., Nies, B., Holzemann, G., Goodman, S. L., and Kessler, H. (2000) Surface coating with cyclic RGD peptides stimulates osteoblast adhesion and proliferation as well as bone formation. *Chembiochem* **1,** 107–114
59. Hansen, L. K., Mooney, D. J., Vacanti, J. P., and Ingber, D. E. (1994) Integrin binding and cell spreading on extracellular matrix act at different points in the cell cycle to promote hepatocyte growth. *Mol. Biol. Cell* **5,** 967–975
60. Bhadriraju, K. and Hansen, L. K. (2000) Hepatocyte adhesion, growth and differentiated function on RGD-containing proteins. *Biomaterials* **21,** 267–272
61. Mooney, D. J., Langer, R., and Ingber, D. E. (1995) Cytoskeletal filament assembly and the control of cell spreading and function by extracellular matrix. *J. Cell Sci.* **108,** 2311–2320
62. Mooney, D., Hansen, L., Vacanti, J., Langer, R., Farmer, S., and Ingber, D. (1992) Switching from differentiation to growth in hepatocytes: control by extracellular matrix. *J. Cell Physiol.* **151,** 497–505
63. Carlisle, E. S., Mariappan, M. R., Nelson, K. D., Thomes, B. E., Timmons, R. B., Constantinescu, A., Eberhart, R. C., and Bankey, P. E. (2000) Enhancing hepatocyte adhesion by pulsed plasma deposition and polyethylene glycol coupling. *Tissue Eng.* **6,** 45–52
64. Park, K. H., Na, K., Kim, S. W., Jung, S. Y., and Chung, H. M. (2005) Phenotype of hepatocyte spheroids behavior within thermo-sensitive poly(NiPAAm-co-PEG-g-GRGDS) hydrogel as a cell delivery vehicle. *Biotechnol. Lett.* **27,** 1081–1086
65. Itle, L. J., Koh, W. G., and Pishko, M. V. (2005) Hepatocyte viability and protein expression within hydrogel microstructures. *Biotechnol. Prog.* **21,** 926–932
66. Pierschbacher, M., Hayman, E. G., and Ruoslahti, E. (1983) Synthetic peptide with cell attachment activity of fibronectin. *Proc. Natl. Acad. Sci. U. S. A.* **80,** 1224–1227
67. Sechler, J. L., Corbett, S. A., and Schwarzbauer, J. E. (1997) Modulatory roles for integrin activation and the synergy site of fibronectin during matrix assembly. *Mol. Biol. Cell* **8,** 2563–2573
68. Danen, E. H., Aota, S., van Kraats, A. A., Yamada, K. M., Ruiter, D. J., and van Muijen, G. N. (1995) Requirement for the synergy site for cell adhesion to fibronectin depends on the activation state of integrin alpha 5 beta 1. *J. Biol. Chem.* **270,** 21612–21618
69. Garcia, A. J., Schwarzbauer, J. E., and Boettiger, D. (2002) Distinct activation states of alpha5beta1 integrin show differential binding to RGD and synergy domains of fibronectin. *Biochemistry* **41,** 9063–9069
70. Cutler, S. M. and Garcia, A. J. (2003) Engineering cell adhesive surfaces that direct integrin alpha5beta1 binding using a recombinant fragment of fibronectin. *Biomaterials* **24,** 1759–70
71. Houseman, B. T., and Mrksich, M. (2001) The microenvironment of immobilized Arg-Gly-Asp peptides is an important determinant of cell adhesion. *Biomaterials* **22,** 943–955
72. Kato, M. and Mrksich, M. (2004) Using model substrates to study the dependence of focal adhesion formation on the affinity of integrin-ligand complexes. *Biochemistry* **43,** 2699–707
73. Kong, H. J., Polte, T. R., Alsberg, E., and Mooney, D. J. (2005) FRET measurements of cell-traction forces and nano-scale clustering of adhesion ligands varied by substrate stiffness. *Proc. Natl. Acad. Sci. U. S. A.* **102,** 4300–4305
74. Aucoin, L., Griffith, C. M., Pleizier, G., Deslandes, Y., and Sheardown, H. (2002) Interactions of corneal epithelial cells and surfaces modified with cell adhesion peptide combinations. *J. Biomater. Sci. Polym. Ed.* **13,** 447–462

75. Merzkirch, C., Davies, N., and Zilla, P. (2001) Engineering of vascular ingrowth matrices: are protein domains an alternative to peptides? *Anat. Rec.* **263,** 379–387
76. Kim, S. H., Hoshiba, T., and Akaike, T. (2003) Effect of carbohydrates attached to polystyrene on hepatocyte morphology on sugar-derivatized polystyrene matrices. *J. Biomed. Mater. Res. A.* **67,** 1351–1359
77. Weigel, P. H. (1980) Rat hepatocytes bind to synthetic galactoside surfaces via a patch of asialoglycoprotein receptors. *J. Cell Biol.* **87,** 855–861
78. Yoon, J. J., Nam, Y. S., Kim, J. H., and Park, T. G. (2002) Surface immobilization of galactose onto aliphatic biodegradable polymers for hepatocyte culture. *Biotechnol. Bioeng.* **78,** 1–10
79. Li, Q., Williams, C. G., Sun, D. D., Wang, J., Leong, K., and Elisseeff, J. H. (2004) Photocrosslinkable polysaccharides based on chondroitin sulfate. *J. Biomed. Mater. Res. A.* **68,** 28–33
80. Nuttelman, C. R., Mortisen, D. J., Henry, S. M., and Anseth, K. S. (2001) Attachment of fibronectin to poly(vinyl alcohol) hydrogels promotes NIH3T3 cell adhesion, proliferation, and migration. *J. Biomed. Mater. Res.* **57,** 217–23
81. Zajaczkowski, M. B., Cukierman, E., Galbraith, C. G., and Yamada, K. M. (2003) Cell-matrix adhesions on poly(vinyl alcohol) hydrogels. *Tissue Eng.* **9,** 525–533
82. Balis, U. J., Behnia, K., Dwarakanath, B., Bhatia, S. N., Sullivan, S. J., Yarmush, M. L., and Toner, M. (1999) Oxygen consumption characteristics of porcine hepatocytes. *Metab. Eng.* **1,** 49–62
83. Catapano, G., De Bartolo, L., Lombardi, C. P., and Drioli, E. (1996) The effect of oxygen transport resistances on the viability and functions of isolated rat hepatocytes. *Int. J. Artif. Organs.* **19,** 61–71
84. Brown, L. A., Arterburn, L. M., Miller, A. P., Cowger, N. L., Hartley, S. M., Andrews, A., Silber, P. M., and Li, A. P. (2003) Maintenance of liver functions in rat hepatocytes cultured as spheroids in a rotating wall vessel. *In Vitro Cell Dev. Biol. Anim.* **39,** 13–20
85. Mann, B. K., Schmedlen, R. H., and West, J. L. (2001) Tethered-TGF-beta increases extracellular matrix production of vascular smooth muscle cells. *Biomaterials* **22,** 439–444
86. Gobin, A. S. and West, J. L. (2003) Effects of epidermal growth factor on fibroblast migration through biomimetic hydrogels. *Biotechnol. Prog.* **19,** 1781–1785
87. Halstenberg, S., Panitch, A., Rizzi, S., Hall, H., and Hubbell, J. A. (2002) Biologically engineered protein-graft-poly(ethylene glycol) hydrogels: a cell adhesive and plasmin-degradable biosynthetic material for tissue repair. *Biomacromolecules* **3,** 710–723
88. Lutolf, M. P., Lauer-Fields, J. L., Schmoekel, H. G., Metters, A. T., Weber, F. E., Fields, G. B., and Hubbell, J. A. (2003) Synthetic matrix metalloproteinase-sensitive hydrogels for the conduction of tissue regeneration: engineering cell-invasion characteristics. *Proc. Natl. Acad. Sci. U. S. A.* **100,** 5413–5418
89. Cruise, G. M., Scharp, D. S., and Hubbell, J. A. (1998) Characterization of permeability and network structure of interfacially photopolymerized poly(ethylene glycol) diacrylate hydrogels. *Biomaterials* **19,** 1287–1294
90. Klein, T. J., Schumacher, B. L., Schmidt, T. A., Li, K. W., Voegtline, M. S., Masuda, K., Thonar, E. J., and Sah, R. L. (2003) Tissue engineering of stratified articular cartilage from chondrocyte subpopulations. *Osteoarthritis. Cartil.* **11,** 595–602
91. Albrecht, D. R., Underhill, G. H., Wassermann, T. B., Sah, R. L., and Bhatia, S. N. (2006) Probing the role of multicellular organization in three-dimensional microenvironments. *Nat. Methods* **3,** 369–375
92. Albrecht, D. R., Tsang, V. L., Sah, R. L., and Bhatia, S. N. (2005) Photo- and electropatterning of hydrogel-encapsulated living cell arrays. *Lab. Chip.* **5,** 111–118

Received for publication August 9, 2006.
Accepted for publication October 11, 2006.